

# Crystallization of a Racemate Affords a $P2_1$ Chiral Crystal Structure: Asymmetric Unit of Two Opposite Handed Molecules Simulates Achiral $P2_1/n$ Packing via Pseudosymmetry

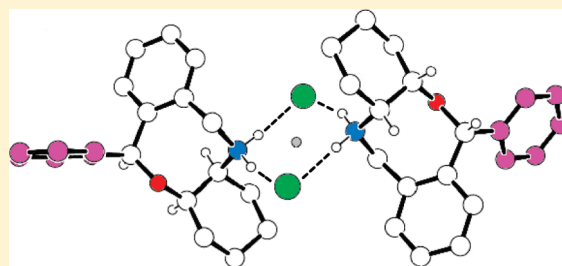
Avital Steinberg,<sup>†</sup> Itzhak Ergaz,<sup>†</sup> Rubén Alfredo Toscano,<sup>‡</sup> and Robert Glaser<sup>\*,‡</sup>

<sup>†</sup>Department of Chemistry, Ben-Gurion University of the Negev, Beer-Sheva 84105, Israel

<sup>‡</sup>Instituto de Química, Universidad Nacional Autónoma de México, Circuito Exterior, C. U., Coyoacán, D.F., 04510, México

 Supporting Information

**ABSTRACT:** A racemic mixture consisting of a secondary ammonium salt ( $\pm$ )-(1*RS*,3*SR*,4*RS*)-1-phenyl-*cis*-3,4-*n*-butano-5,6-dihydro-1*H*-2,5-benzoxazocine hydrochloride (**1**) crystallized as a “false conglomerate” of crystals in the monoclinic system, Sohncke space group  $P2_1$  with two molecules of opposite handedness in the asymmetric unit and at 295(2) K:  $a = 10.224(2)$  Å,  $b = 13.969(2)$  Å,  $c = 12.724(2)$  Å,  $\beta = 98.996(2)^\circ$ ,  $V = 1794.9(5)$  Å<sup>3</sup>,  $Z = 4$ , and  $Z' = 2$ . The *cis*-3,4-*n*-butano-5,6-dihydro-1*H*-2,5-benzoxazocine fused-ring skeletons are approximately enantiotopic and exhibit pseudo-inversion and pseudo-*n*-glide relationships. These noncrystallographic symmetries enable space filling in the chiral crystal structure to resemble that of a higher order achiral  $P2_1/n$  apparent space group ( $Z = 4$ ,  $Z' = 1$ ). The secondary ammonium salt molecules crystallize in patterns influenced by a complex blend of N–H $\cdots$ Cl, C–H $\cdots$ Cl, C–H $\cdots$ O, and C–H $\cdots$ Ar interactions that seem to be responsible for different conformational twists of the phenyl rings in the structure. Avnir's CSM method was adapted for quantification of crystallographic pseudosymmetry. RmS(*G*) measurements of distortion from ideal *G* symmetries were developed for pure translation, screw rotation, and glide reflection, as well as point group symmetries. Low rmS(*i*) and rmS(*n*-glide) values show high fidelity for the emulation of  $P2_1/n$  space filling in crystalline **1**.



## INTRODUCTION

About 90% of the time, crystallization of a racemic mixture of organic compounds yields achiral crystals known as *racemic compounds* in the solid-state.<sup>1</sup> The achiral crystal lattice contains equal quantities of both enantiomers that reside in well-defined positions.<sup>2</sup> On the other hand, only about 10% of all racemic mixtures of organic compounds crystallize as *conglomerates of chiral crystals*.<sup>1</sup> These are simple mechanical mixtures of (+)- and (–)-chiral crystals in a 1:1 statistical ratio.<sup>2</sup> Usually, only one molecule resides in the asymmetric unit ( $Z' = 1$ ) of these chiral crystals. Dissolution of one crystal excised out of the bulk results in a solution containing an enantiomerically pure compound.

Desiraju<sup>3</sup> has noted that during the period of 1970–2006, the percentage of organic compounds in the Cambridge Structural Database<sup>4</sup> with more than one molecule in the asymmetric unit has remained virtually constant at approximately 11%. Two molecules in the asymmetric unit ( $Z' = 2$ ) occur when it is difficult, by symmetry alone, to simultaneously satisfy both the criteria of close packing and the requirements of optimal intermolecular interactions.<sup>5</sup> This situation enables the intriguing possibility of two molecules of either invariant or opposite handedness comprising the asymmetric units of these chiral crystal structures. In most of those cases asymmetric units consist of two molecules with the same handedness. Bishop and Scudder<sup>6</sup> have referred to conglomerates of chiral crystals containing two symmetry

unrelated molecules of opposite handedness as *false conglomerates*. They estimate the frequency for false conglomerate formation to be about 1% for organic compounds.<sup>6</sup> False conglomerates differ from true conglomerates in that dissolution of one chiral crystal excised out of the bulk will now produce an optically inactive solution of solvated enantiomers.

It is very common for both independent molecules to exhibit the same (but not identical) conformation, and when they do, then their corresponding bond lengths, angles, and torsion angles are usually statistically similar.<sup>5</sup> However, it is the relative energies of conformations and packing considerations that ultimately determine if one or multiple conformations are to be found in the  $Z' > 1$  asymmetric unit. When the conformations are the same, it is often possible to show that the independent molecules are related to one another by approximate symmetry transformations (pseudosymmetry).<sup>5</sup> Pseudosymmetrical independent molecules in the asymmetric unit implies that structurally similar diastereomers mimic pairs of homomers or enantiomers and show a particular intermolecular spatial orientation approximating symmetry. Gavezzotti<sup>7</sup> has investigated a large population of crystals with two molecules in the asymmetric unit ( $Z' = 2$ ) and noted that with an asymmetry tolerance of 0.5 Å

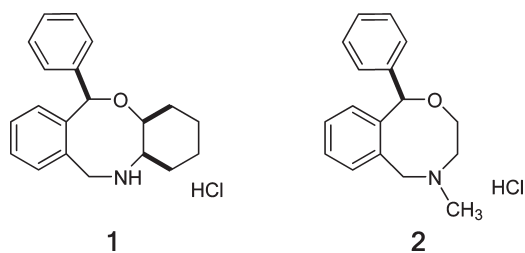
**Received:** November 10, 2010

**Revised:** February 22, 2011

**Published:** March 21, 2011

atom<sup>-1</sup>, 83% of the nonsymmetry related molecular arrangements in the asymmetric unit revealed some kind of noncrystallographic symmetry beyond that of the true symmetry imposed by the space group. The presence of crystallographic pseudosymmetry emphasizes that the "...preconception that symmetry must rule exact and uninterrupted throughout proper crystals for best packing and for thermodynamic stability"<sup>7</sup> sometimes is only achieved via multiple content ( $Z' > 1$ ).

This paper describes the crystal packing within a false conglomerate produced via crystallization of a racemic mixture of the secondary ammonium salt ( $\pm$ )-(1*RS*,3*SR*,4*RS*)-1-phenyl-*cis*-3,4-*n*-butano-5,6-dihydro-1*H*-2,5-benzoxazocine hydrochloride (*N*-desmethyl-*cis*-3,4-*n*-butano-nefopam HCl, **1**). The oppositely handed fused-ring skeletons in these chiral crystals exhibit pseudoinversion and pseudo-*n*-glide reflection relationships. The crucial role of pseudosymmetry in space filling within the false conglomerate will be discussed in this report.



Avnir and co-workers have shown that chirality and distortion from ideal symmetry and from ideal shape should be considered to be continuous properties. These have been quantified by Continuous Symmetry Measures (CSM),<sup>8–14</sup> Continuous Chirality Measures,<sup>15</sup> and Continuous Shape Measures (CShM).<sup>16,17</sup> The CSM of a structure is a normalized root-mean-square (rms) distance function from the closest theoretical structure which has the ideal symmetry.<sup>8,9,11,14</sup> The broad utility of the Avnir Continuous Symmetry Measures has been extensively demonstrated for quantification of symmetry distortion within objects/molecules, and has led to correlations of these values for a wide range of physico-chemical phenomena,<sup>18–23</sup> and even anthropology.<sup>24</sup> The application of Symmetry Operation Measures to inorganic chemistry,<sup>25</sup> and the use of CShM<sup>25–29</sup> measurements for analysis of complex polyhedral structures has also been discussed by Alvarez and co-workers.

The fidelity of a pseudosymmetry relationship is a variable which can be quantified, and its values should represent a continuum. A number of measurements for pseudosymmetry in crystals may be found in the literature.<sup>7,30–33</sup> Avnir's CSM method is unique because it can treat two pseudosymmetric molecules (or corresponding subunits in two molecules) as one ensemble unit and calculate a root-mean-square (rms) distance from the closest theoretical ensemble which has the specified symmetry. A desire to calculate a single parameter value for the fidelity of the intermolecular pseudosymmetry relationships in this crystal prompted us to modify and extend the Continuous Symmetry Measures of Avnir and co-workers. The classical CSM measurements were based on distortion from ideal point group symmetries, and thus they had to be modified for symmetry operations with translation components observed solely in space groups, that is, pure translation, glide-reflection (reflection-translation), and screw-rotation (rotation-

translation). The quantification of the pseudosymmetry operations in this crystal will also be discussed below.

## EXPERIMENTAL SECTION

**NMR Spectroscopy.** Solution-state <sup>1</sup>H and <sup>13</sup>C NMR spectroscopy were recorded at ambient temperature on a spectrometer at 500.13 and 125.76 MHz, respectively. The sample was measured in CD<sub>2</sub>Cl<sub>2</sub> using the deuterium solvent as an internal lock. <sup>13</sup>C and <sup>1</sup>H chemical shifts were based on the respective CD<sub>2</sub>Cl<sub>2</sub> [53.8 ppm] and residual CHDCl<sub>2</sub> [5.32 ppm] signals as internal references. Homonuclear decoupling was used to assign the spin–spin coupling constants. The DEPT-135 pulse-sequence was used to ascertain the hydrogen multiplicity of the <sup>13</sup>C signals. HMQC 2D-NMR spectroscopy was used to correlate the <sup>13</sup>C and <sup>1</sup>H chemical shifts. NOE-DIFF experiments were performed to aid in signal assignment.

( $\pm$ )-(1*RS*,3*SR*,4*RS*)-1-Phenyl-*cis*-3,4-*n*-butano-5,6-dihydro-1*H*-2,5-benzoxazocine Hydrochloride (**1**). Using the method of Glaser et al.<sup>34</sup> for the analogous preparation of *N*-desmethylnefopam HCl, phenylmagnesium bromide was reacted with phthalaldehyde in cold dried ether to give the 2-hydroxy-5-phenyl-2,5-dihydro-3,4-benzofuran crystalline intermediate (mp 120–122 °C). Reaction of this intermediate with *cis*-2-aminocyclohexanol (from Acros Organics Inc.) in warm toluene afforded *cis*-2-(3-phenyl-1,3-dihydro-isobenzofuran-1-ylamino)-cyclohexanol as a crude intermediate which was then reduced by LiAlH<sub>4</sub> to give *cis*-2-(2-hydroxy-cyclohexane)-aminomethylbenzhydrol as a crystalline intermediate [mp 100–103°]. Ring closure of the benzhydrol with *p*-CH<sub>3</sub>C<sub>6</sub>H<sub>4</sub>SO<sub>2</sub>OH/toluene and workup gave a crude viscous oil containing a 1:10 mixture of (1*RS*,3*RS*,4*SR*)- and (1*RS*,3*SR*,4*RS*)-1-phenyl-*cis*-3,4-*n*-butano-5,6-dihydro-1*H*-2,5-benzoxazocine (*cis*-3,4-*n*-butano-*N*-desmethylnefopam) free base diastereomers. After dissolving the oil in ether and a few drops of methanol, ethereal HCl was carefully added dropwise until acidic to pH paper to yield a solid that was recrystallized from methanol/ethyl acetate/*n*-hexane to afford 1.4 g (73% yield) ( $\pm$ )-(1*RS*,3*SR*,4*RS*)-1-phenyl-*cis*-3,4-*n*-butano-5,6-dihydro-1*H*-2,5-benzoxazocine hydrochloride (**1**), mp 259–261 °C; IR (KBr)  $\nu$  3416 cm<sup>-1</sup> (NH); <sup>1</sup>H NMR (CD<sub>2</sub>Cl<sub>2</sub>)  $\delta$  5.77 [s, 1H, H(1)], 4.02 [dt,  $J(3ax-4eq) = 2.9(3)$  Hz,  $J(3ax-19eq) = 3.6(5)$  Hz,  $J(3ax-19ax) = 9.6(1)$  Hz, 1H, H(3ax)], 3.52 [dt,  $J(3ax-4eq) = 2.9(3)$  Hz,  $J(4eq-22eq) = 3.5(2)$  Hz,  $J(4eq-22ax) = 6.5(2)$  Hz, 1H, H(4eq)], 7.77 [broad-s, 1H, NH(S)], 7.91 [broad-s, 1H, NH(S')], 5.39 [d,  $J = -12.6$  Hz, 1H, H(6endo)], 4.25 [d,  $J = -12.6$  Hz, 1H, H(6exo)], 7.54 [dd,  $J(7-8) = 6.3$  Hz,  $J(7-9) = 2.9$  Hz, 1H, H(7)], 7.16 [dd,  $J(9-10) = 6.2$  Hz,  $J(8-10) = 2.9$  Hz, 1H, H(10)], 7.22–7.36 [m, 7H, ArH], 2.14 [m, 1H, H(19ax)], 1.77 [m, 1H, H(19eq)], 1.42 [m, 1H, H(20ax)], 1.87 [m, 1H, H(20eq)], 1.97 [m, 1H, H(21ax)], 1.54 [m, 1H, H(21eq)], 2.22 [m, 1H, H(22ax)], 1.77 [m, 1H, H(22eq)]; <sup>13</sup>C{<sup>1</sup>H} NMR (CD<sub>2</sub>Cl<sub>2</sub>)  $\delta$  85.28 [C(1)], 77.51 [C(3), broad], 52.79 [C(4)], 47.51 [C(6)], 134.82 [C(7)], 128.77 [C(10)], 29.03 [C(19)], 22.77 [C(20)], 21.47 [C(21)], 25.99 [C(22)]; 129.76, 128.35, 128.12, 127.65 [unassigned ArCH]; 143.04, 142.63 [ArC(quat)]. Anal. Calcd for C<sub>20</sub>H<sub>24</sub>ClNO: C, 72.82; H, 7.33; N, 4.25. Found: C, 72.54; H, 7.41; N, 4.03. See Supporting Information for complete details of the synthesis procedure.

**X-ray Crystallography of ( $\pm$ )-(1*RS*,3*SR*,4*RS*)-1-Phenyl-*cis*-3,4-*n*-butano-5,6-dihydro-1*H*-2,5-benzoxazocine Hydrochloride (**1**).**<sup>35</sup> Crystallization was performed by vapor diffusion of *n*-hexane into a methanol/ethyl acetate solution of salt **1**. A clear prism of C<sub>20</sub>H<sub>24</sub>ClNO having the approximate dimensions of 0.89 × 0.52 × 0.44 mm<sup>3</sup> was chosen, mounted on a glass fiber, and then fixed to the goniometer head of the X-ray diffractometer. Crystallographic measurements were made on a Bruker SMART 1k CCD diffractometer with graphite monochromated Mo K $\alpha$  ( $\lambda = 0.71073$  Å) radiation. Data were collected to a maximum  $\theta$  value of 23.45° (96.7% completeness to  $\theta$ ), and then reduced by the SAINT<sup>36</sup> software package. Analysis of the data

showed negligible decay during data collection, the intensities were corrected for Lorentz and polarization factors, and an empirical absorption correction was applied via SADABS<sup>37</sup> ( $T_{\min}$  0.8778,  $T_{\max}$  1.0000). The structure was solved by application of direct methods and refined by full matrix least-squares on  $F^2$  using the SHELXTL<sup>38</sup> software package. Cell constants corresponded to a monoclinic system with dimensions at 295(2) K of  $a = 10.224(2)$  Å,  $b = 13.969(2)$  Å,  $c = 12.724(2)$  Å,  $\beta = 98.996(2)^\circ$ , and  $V = 1794.9(5)$  Å<sup>3</sup>. Systematic absences correspond to either  $P2_1$  (noncentrosymmetric) or  $P2_1/m$  (centrosymmetric) space groups. Attempts to solve the structure in the centrosymmetric space group  $P2_1/m$  were uniformly unsuccessful, but the structure solved immediately in  $P2_1$  and refined to a final  $R = 0.0241$ . Refinement in the centrosymmetric space group  $P2_1/n$  (one molecule in the asymmetric unit) was carried out after the proper origin shift. The refinement and the molecular packing arrangement showed that the pseudoinversion centers and pseudo- $n$ -glide reflection planes are only local pseudosymmetry elements. We conclude that the space group is unambiguously  $P2_1$ . For  $Z = 4$ ,  $Z' = 2$  and  $fw = 329.85$ , the calculated density is 1.221 g/cm<sup>3</sup>. 7556 reflections were measured, 3885 unique, ( $R_{\text{int}} = 0.0151$ ). Hydrogens attached to N-atoms were located in the difference Fourier map and refined isotropically. The rest of the H-atoms in this structure were introduced at calculated positions as riding atoms, with C–H = 0.98 Å (CH), 0.97 Å (CH<sub>2</sub>), or 0.93 Å (aromatic) and  $U_{\text{iso}}(\text{H}) = 1.2U_{\text{eq}}(\text{C})$ . All non-hydrogen atoms were refined anisotropically. At convergence, the final discrepancy indices on  $F$  were  $R(F) = 0.0241$ ,  $R_w(F^2) = 0.0596$ , and GOF  $S = 1.015$  for the 3885 reflections with  $I_{\text{net}} > 2\sigma(I_{\text{net}})$  and 431 parameters refined with 1 constraint. The residual negative and positive electron densities in the final map were  $-0.133$  and  $0.117$  e/Å<sup>3</sup>. The handedness of the polar structure was determined by successful refinement of the Flack parameter ( $-0.06(4)$ ).

**The rms(G) Pseudosymmetry Tool, Where  $G = i, \sigma, C_n$ , and  $S_n$ .** CSM calculations were performed at the Web site<sup>39</sup> of the Avnir group at the Hebrew University of Jerusalem, using the Advanced mode. Input file format information and a tutorial are provided at the site. These calculations include the deviation from ideal  $G$  point group symmetries of  $G = i, \sigma, C_n$ , and  $S_n$ . The fractional coordinates of an ensemble consisting of  $G$  pseudosymmetry related  $n$ -pairs of atoms within two molecules/or fragments were converted to Cartesian space and then arranged in an MDL (\*.mol format) input file. Another input file specifies the permutation of atom pairs for the desired  $G$  pseudosymmetry relationship. The coordinates of the theoretical ‘nearest ideal geometrical ensemble’ having bona fide  $G$  symmetry<sup>8,9,11,14</sup> were calculated from the input coordinates using the appropriate Avnir CSM algorithm.<sup>39</sup> The size-dependent CSM  $S(G)$  value, scaling factor, initial ensemble (structure) coordinates, resulting ideal  $G$ -symmetry ensemble (structure) coordinates, directional cosines and the atom permutation list appear in the output “Results” file.<sup>39</sup> Then, atoms in the “nearest ideal  $G$  symmetry ensemble of geometrical structures” were superimposed upon corresponding atoms in the input ensemble of a  $G$  pseudosymmetry related pair of molecules/or fragments to give the rms interatomic distance. This is an average deviation from ideal  $G$  symmetry which is defined as a crystallographic  $G$  pseudosymmetry measure called “the nonsize normalized rms( $G$ ) tool”.

**Location of Statistically Determined Pseudosymmetry Elements.** The midpoints (i.e., average coordinates)  $[\bar{x}_i\bar{y}_i\bar{z}_i]$  between corresponding  $n$ -pairs of atoms within the approximately enantiomeric fused-ring skeletons of the (+)-A and (–)-B molecules generate either a cluster of points (see Figure 1), or an approximately linear string of points (not applicable for crystalline 1) or an almost planar array of points, if the fragments are related by pseudoinversion, or pseudo- $2_1$  screw-rotation, or pseudoglide reflection, respectively. The  $x_{\text{mean}}$  value for all the midpoints between  $n$ -pairs of pseudoinversion symmetry

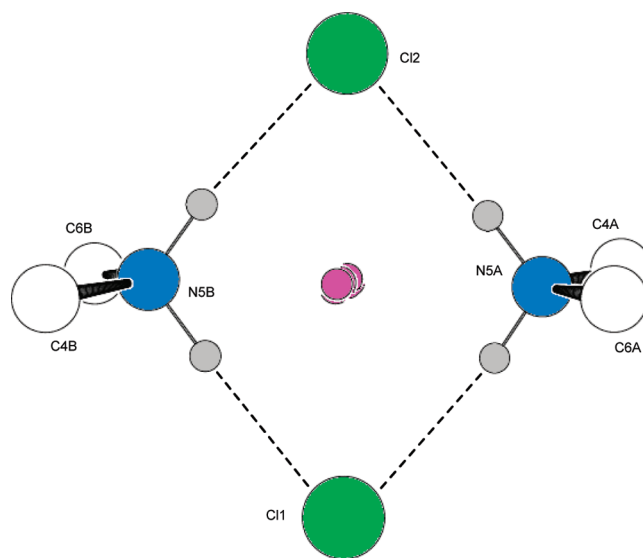


**Figure 1.** Cluster of magenta colored graphically enlarged midpoints (i.e., average coordinates)  $[\bar{x}_i\bar{y}_i\bar{z}_i]$  between corresponding  $n$ -pairs of atoms within the approximately enantiomeric fused-ring skeletons of the (+)-A and (–)-B molecules (1). For simplicity, only the nitrogens and their ligated atoms have been illustrated for each molecule. Broken lines indicate hydrogen bonds.

related atoms in molecules A and B is:

$$x_{\text{mean}} = \frac{\sum_{i=1}^n \bar{x}_i}{n}$$

The point defined by the  $[x_{\text{mean}}, y_{\text{mean}}, z_{\text{mean}}]$  fractional coordinates is the statistical “best point”, and its estimated standard deviation (esd) is the precision of this value. A statistically calculated “best line” or “best plane” can be calculated from the set of midpoint  $[\bar{x}_i\bar{y}_i\bar{z}_i]$  coordinates between corresponding  $n$ -pairs of atoms in pseudoscrew and pseudoglide arrays of points using modules developed for MATLAB.<sup>40,41</sup>

**Pseudo-Glide Translation.** A crystallographic glide symmetry operation is a composite of a translation and a reflection. If the directional cosine values of the  $\alpha$ ,  $\beta$ , and  $\gamma$  angles, which the “normal to the best plane”<sup>42</sup> make with the positive directions of the coordinate axes show that these lines are parallel to a cell face, then one is justified in treating the glide reflection pseudosymmetries as separate translation and reflection components, respectively (a similar argument can be made for a pseudo- $2_1$  screw rotation ‘best line’<sup>41</sup> which is parallel to a cell axis). After molecule (–)-B is translated along the ‘best glide’ translation line, it has a pseudo mirror relationship with respect to molecule (+)-A that can be quantified using the rms( $\sigma$ ) tool. Similarly for a pseudo- $2_1$  screw rotation relationship, if molecule (–)-B is translated along the ‘best screw’ translation line, it will now have a pseudo- $C_2$  rotation arrangement relative to molecule (+)-A whose fidelity can be quantified using the rms( $C_2$ ) tool. In the crystal under consideration, the ‘best pseudo- $n$ -glide translation line’ lies within one of two  $ac$ -planes. Therefore, they each are composed of an  $x$ -component and a  $z$ -component. The  $x_i$ -translation of an atom in molecule (–)-B with respect to one in molecule (+)-A can be calculated from the difference in their respective  $x_i$  fractional coordinates, for example,  $\Delta x_i = x_i(\text{A}) - x_i(\text{B})$ . A  $\Delta z_i$  value can be calculated in a similar fashion.

**The rms(translation) Pseudosymmetry Tool.** An ideal translation  $\Delta x_i$  value would obviously be exactly 0.5 fractional coordinate units. The difference between an actual  $x_i$ -translation ( $\Delta x_i$ ) minus the ideal value for a bona fide glide reflection (or  $2_1$  screw-rotation) is calculated for each of the  $n$ -pairs of atoms in the ensemble. The rms value

**Table 1.** Selected Torsion Angles [°] for Eight-Membered Ring Boat–Boat Conformation and Phenyl Twist in (1*R*,3*S*,4*R*)-A (1A) and (1*S*,3*R*,4*S*)-B (1B) versus (1*S*)-Nefopam HCl (2)

torsion angle	molecule A	molecule B	2
C(11)–C(1)–O(2)–C(3)	85.7(2)	–82.7(2)	–82.74
C(1)–O(2)–C(3)–C(4)	–70.3(2)	71.5(2)	63.82
O(2)–C(3)–C(4)–N(5)	–50.5(2)	49.7(2)	57.87
C(3)–C(4)–N(5)–C(6)	59.8(2)	–61.9(2)	–59.29
C(4)–N(5)–C(6)–C(12)	46.4(3)	–43.3(3)	–49.15
N(5)–C(6)–C(12)–C(11)	–81.1(3)	81.8(3)	79.09
C(6)–C(12)–C(11)–C(1)	2.1(3)	–1.9(3)	3.23
C(12)–C(11)–C(1)–O(2)	5.9(3)	–9.0(3)	–6.56
C(11)–C(1)–C(13)–C(18)	20.1(2)	–77.8(2)	–65.77
H(1)–C(1)–C(13)–C(14)	–42.8	–16.5	–4.2

for the set of  $n$ -differences is the deviation from an ideal  $x_r$ -translation (in fractional coordinates) along the corresponding direction,  $\text{rms}(x\text{-translation})_{\text{coordinate}}$ :

$$\text{rms}(x\text{-translation})_{\text{coordinate}} = \sqrt{\frac{\sum_{i=1}^n (\Delta x_i - 0.5)^2}{n}}$$

The  $\text{rms}(x\text{-translation})_{\text{coordinate}}$  value was multiplied by the  $a$ -axis cell length to give the relevant crystallographic translation pseudosymmetry measure,  $\text{rms}(x\text{-translation})$  now in Å.

#### The $\text{rms}(\text{glide})$ and $\text{rms}(\text{screw})$ Pseudosymmetry Tools.

The  $x_{\text{mean}}$ -translation (or  $y_{\text{mean}}$ -translation, not applicable for 1) or  $z_{\text{mean}}$ -translation is the mean value of the  $\Delta x_i$  (or  $\Delta y_i$ ) or  $\Delta z_i$  fractional coordinate distances between the  $n$ -pairs of atoms involved in a translation of molecule (–)-B to (+)-A. For example

$$x\text{-translation}_{\text{mean}} = \frac{\sum_{i=1}^n \Delta x_i}{n}$$

If statistically insufficient midpoints are present in one unit cell to calculate a “best line” or “best plane” that is parallel to a cell face, then midpoints from adjacent unit cells should be added to the set. For a pseudo  $n$ -glide in crystalline 1, a ‘dummy’ molecule (–)-B was created from (–)-B by transforming its atomic coordinates by the respective  $x_{\text{mean}}$  and  $z_{\text{mean}}$  values so that it was opposite (+)-A. Now, from an input file of the Cartesian coordinates of the ensemble of “dummy”-B and actual A molecules, the coordinates of the closest theoretical geometrical structure with bona fide reflection symmetry was calculated with the Avnir CSM  $S(\sigma)$  program. The nondistance dependent deviation from true reflection symmetry in the “dummy” (–)-B plus actual (+)-A ensemble of molecules [ $\text{rms}(\sigma)_{\text{glide}}$ ] was calculated in a similar manner to  $\text{rms}(\sigma)$  described above. The  $\text{rms}(\text{glide})$  is the summation of its two components:  $\text{rms}(\sigma)_{\text{glide}} + \text{rms}(\text{translation})_{\text{glide}}$ , and their values are in Å. If a pseudo- $2_1$  screw relationship exists within the ensemble of ‘dummy’ and real molecules, then  $\text{rms}(C_2)_{\text{screw}}$  is calculated by analogy to  $\text{rms}(C_2)$  also described above, and  $\text{rms}(\text{screw})$  equals  $\text{rms}(C_2)_{\text{screw}} + \text{rms}(\text{translation})_{\text{screw}}$ .

**CSM Error Estimation.** The errors in the CSM values are estimated using the Avnir CSM Error Estimation Program, which takes the number of unique reflections, the thermal factors, and the CSM value into account as input, and returns a CSM range or an upper bound for the CSM values.<sup>12</sup>

## RESULTS AND DISCUSSION

The *cis*-3,4-*n*-butano-5,6-dihydro-1*H*-2,5-benzoxazocine fused-ring skeletons in the  $P2_1$  crystal are ‘almost enantiomeric’ in structure and the eight-membered rings therein have *boat–boat* (BB) conformations that are both very similar to that observed for the parent non-narcotic analgesic drug ( $\pm$ )-nefopam HCl (2),<sup>42</sup> see selected torsion angles in Table 1. The close geometrical similarity of the skeletons in salt 1 is seen by inverting the handedness of one of them followed by superimposition of all corresponding non-hydrogen atoms (but no phenyl atoms) to give a very small root mean squared (rms) difference of only 0.051 Å. A striking feature of the crystal structure is that the phenyl rings ligated to each skeleton have different twist conformations (angle between planes = 60.1°). One phenyl ring C(18A<sub>ortho</sub>) almost eclipses a benzo-ring C(11A<sub>ipso</sub>) sp<sup>2</sup>-carbon in molecule A [C(11A)–C(1A)–C(13A)–C(18A) + 20.1°], while C(14B<sub>ortho</sub>) in the other phenyl ring approximately eclipses an H(1B<sub>benzhydrylic</sub>) proton in molecule B [H(1B)–C(1B)–C(13B)–C(14B) – 16.5°]. The phenyl ring also eclipses the benzhydrylic-H in the crystalline parent drug (2).

For the sake of simplicity, the two molecules will be arbitrarily referred to as (+)-A and (–)-B, respectively. These molecules crystallize in patterns influenced by a complex blend of N–H⋯Cl, C–H⋯Cl, C–H⋯O, and C–H⋯Ar interactions. An  $R^2_4(8)$  ring hydrogen-bonding pattern graph set<sup>43</sup> involves 2 hydrogen-bond acceptors and 4 hydrogen-bond donors in an 8-atom ring cycle that links all pairs of (1*R*,3*S*,4*R*)-A and (1*S*,3*R*,4*S*)-B molecules (see Figures 1–3). In this ring pattern, N(5A)–H(5A)⋯Cl(1) 2.30(2) Å, N(5A)–H(5B)⋯Cl(2) 2.18(3) Å, N(5B)–H(5C)⋯Cl(2) 2.21(3) Å, and N(5B)–H(5D)⋯Cl(1) 2.14(3) Å, while the corresponding N–H⋯Cl angles are: 153(2)°, 175(2)°, 159(2)°, and 170(2)°. The hydrogen-bonding interactions involve the pseudoinversion symmetry related and more sterically demanding fused-ring pseudoenantiomeric ‘skeletal’ fragments of the diastereomers.

These heterodimers extend the structure into infinite chains along the  $b$ -direction by C–H⋯Cl interactions {C(16A)–H(16A)⋯Cl(2)[ $x, -1 + y, z$ ] 2.97 Å and C(16B)–H(16B)⋯Cl(1)[ $x, 1 + y, z$ ] 3.11 Å}. Parallel chains generated by  $2_1$  symmetry operations are held together by C–H⋯Cl interactions {C(8A)–H(8A)⋯Cl(1)[ $-1 + x, y, z$ ] 2.78 Å and C(8B)–H(8B)⋯Cl(2)[ $1 - x, 1/2 + y, 1 - z$ ] 2.83 Å} giving rise to extra C–H⋯O interactions {C(17B)–H(17B)⋯O(2A)[ $x, 1 + y, z$ ] 2.62 Å} and C(aryl)–H⋯ $\pi$  interactions {C(15A)–H(15A)⋯Aryl-C(7A→12A)<sub>centroid</sub>[ $2 - x, -1/2 + y, -z$ ] 2.83 Å, and C(15B)–H(15B)⋯Aryl-C(7B→12B)<sub>centroid</sub>[ $1 - x, 1/2 + y, 1 - z$ ] 2.87 Å}, which in turn seem to be responsible for the different orientations of the phenyl rings in the structure, see Figure 3.

**Pseudoinversion Symmetry.** Figure 2 clearly depicts a pseudoinversion relationship between the fused-ring skeletons of molecule (+)-A and molecule (–)-B if the disparately twisted phenyl rings are overlooked. If the inversion was bona fide, then the [ $\bar{x}, \bar{y}, \bar{z}$ ] midpoints between pairs of corresponding atoms in the two molecules would all converge at one single point located at a specific spatial location in the crystal lattice (a *special position of inversion symmetry*). But, since pseudosymmetry between oppositely handed diastereomeric (rather than enantiomeric) skeletons is involved, then the distribution of midpoints becomes a cluster of points occupying a *general position of symmetry*, where local site symmetry is only identity (see enlargement in Figure 1).

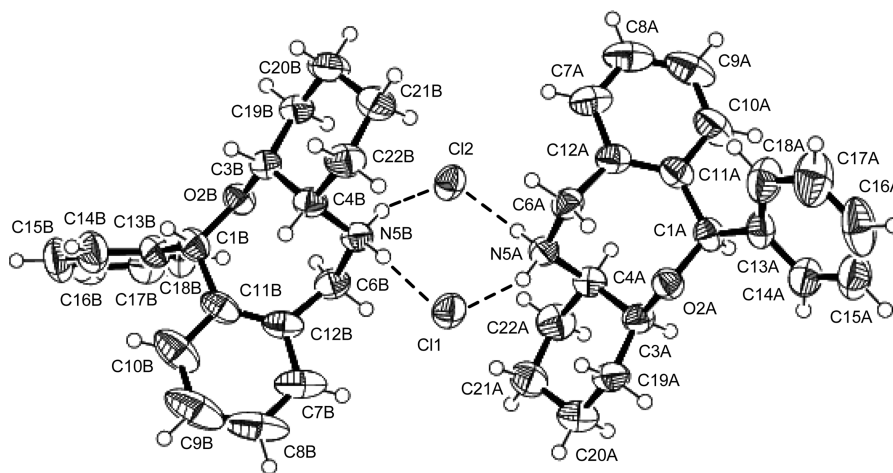


**Figure 2.** Molecular structure, numbering diagram, and hydrogen-bond pattern for (1*R*,3*S*,4*R*)-**A** and (1*S*,3*R*,4*S*)-**B** in the asymmetric unit of  $P2_1$  salt **1**. Displacement ellipsoids are drawn at the 50% probability level. Broken lines indicate hydrogen bonds. A statistically determined 'best point' of pseudoinversion at coordinates [0.779(3),0.501(2),0.249(4)] lies near the center of the  $R_4^2(8)$  ring hydrogen-bonding pattern graph set.

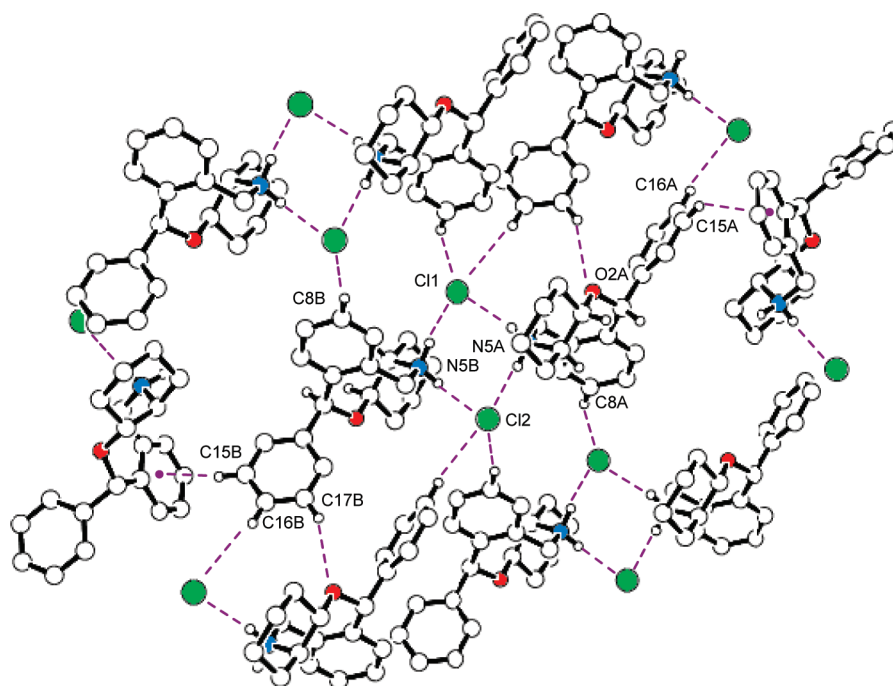


**Figure 3.** The heterodimers extend the structure into infinite chains along the *b*-direction by C(16*A*)—H(16*A*)⋯Cl(2) and C(16*B*)—H(16*B*)⋯Cl(1) interactions. Parallel chains generated by  $2_1$  symmetry operations are held together by a complex blend of C—H⋯Cl, C—H⋯O, and C—H⋯Ar interactions which seem to be responsible for the different orientations of the phenyl rings in the structure.

The location of the above-mentioned pseudoinversion cluster of points is a statistically determined [ $x_{\text{mean}}, y_{\text{mean}}, z_{\text{mean}}$ ] best point at coordinates [0.779(3),0.501(2),0.249(4)]. The estimated standard deviation of these coordinates is the precision of the pseudosymmetry inversion cluster.

The  $2_1$  screw-rotation operator generates (+)-**A**[1 - *x*, *y* + 0.5, 1 - *z*] and (-)-**B**[1 - *x*, *y* - 0.5, 1 - *z*], the remaining two molecules within the unit cell. An additional pseudoinversion relationship exists between their fused-ring skeletons (i.e., again neglecting the phenyls), see Figure 4. Now, the coordinates of the statistically determined best point are [0.221(3), 0.501(2), 0.751(4)], about midway between the edge-to-face phenyl rings.

Once again, the different phenyl-ring twists of the aromatic edge-to-face<sup>44</sup> interaction (centroid⋯centroid 4.84 Å) break bona fide inversion symmetry, but this is dismissed when discussing pseudoinversion between the larger fused-ring skeletal fragments. Within the unit cell are two additional pseudoinversion relationships. Each involves one of the two (-)-**B** molecules from within the unit cell plus a nearby (+)-**A** molecule in an adjacent cell: Figure 5 shows molecules (-)-**B** and (+)-**A**[*x* - 1, *y*, *z*] whose statistical best point is [0.279(3), 0.501(2), 0.249(4)], and Figure 6 depicts the molecules (-)-**B**[1 - *x*, *y* - 0.5, 1 - *z*] and (+)-**A**[2 - *x*, *y* + 0.5, 1 - *z*] whose statistical best point is [0.721(3), 0.501(2), 0.751(4)].

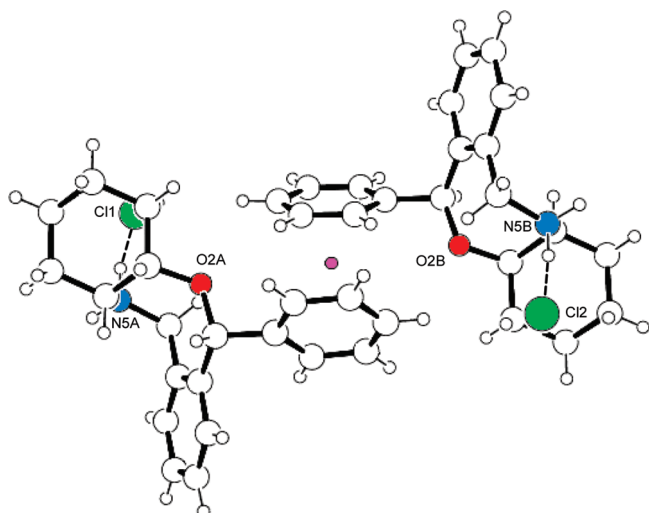


**Figure 4.** An edge-to-face phenyl–phenyl interaction (centroid···centroid 4.84 Å) between the  $2_1$ -screw generated molecules (+)-A[1 -  $x$ ,  $y$  + 0.5, 1 -  $z$ ] on the left and (-)-B[1 -  $x$ ,  $y$  - 0.5, 1 -  $z$ ] on the right. A statistically determined best point of pseudoinversion for the fused-ring skeletons is between the asymmetrically arranged phenyls and has coordinates [0.221(3), 0.501(2), 0.751(4)].

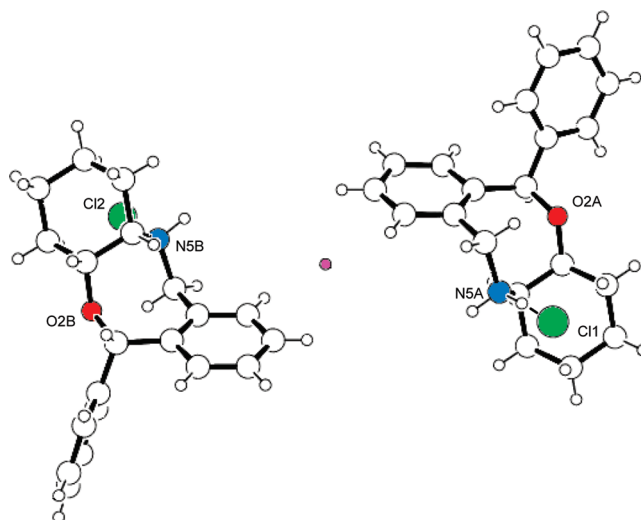


**Figure 6.** Statistically determined best point of pseudoinversion for the fused-ring skeletons of molecules (+)-A[2 -  $x$ ,  $y$  + 0.5, 1 -  $z$ ] on the right and (-)-B[1 -  $x$ ,  $y$  - 0.5, 1 -  $z$ ] on the left is at coordinates [0.721(3), 0.501(2), 0.751(4)].

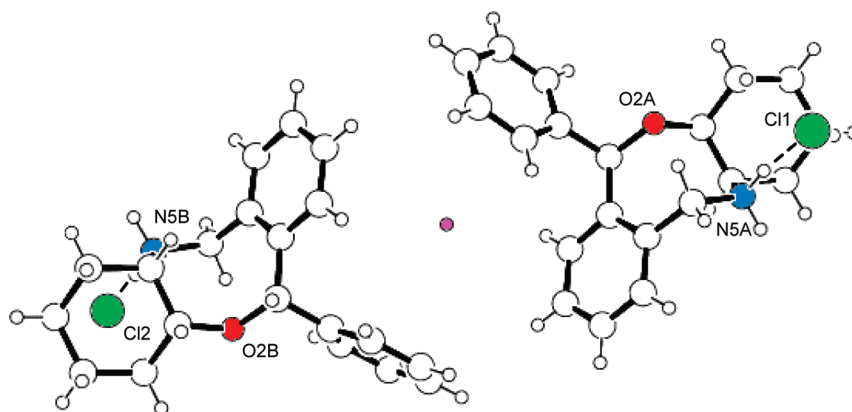


**Figure 5.** Statistically determined best point of pseudoinversion for the fused-ring skeletons in molecules (+)-A[ $x$  - 1,  $y$ ,  $z$ ] on the right and (-)-B on the left is at coordinates [0.279(3), 0.501(2), 0.249(4)].

**Measures for Crystallographic Pseudosymmetry.** Pseudosymmetry measurements were confined to ensembles of two fused-ring skeletal fragments since only they are capable of showing intermolecular symmetry. When the Avnir CSM  $S(i)$  calculation was used to measure the departure from true inversion within the four ensembles of two pseudoenantiomeric skeletons (i.e., neglecting the phenyls) depicted in Figures 2 and 4–6, the results varied from 0.020 to 0.040 (where ideal inversion symmetry is  $S(i) = \text{integer zero}$ ). Despite the fact that there can be no symmetry (and thus no pseudosymmetry) between the edge-to-face phenyls due to their asymmetric arrangement,  $S(i)$  was calculated for four ensembles of just phenyl pairs in order to provide comparative numerical values when inversion symmetry was impossible. The closer the two noninversion related phenyl rings were to each other, the higher was their  $S(i)$  value:  $S(i) = 2.64(1)$  (Figure 4, centroid···centroid 4.84 Å),  $S(i) = 1.37(1)$  (Figure 5, centroid···centroid 7.18 Å),  $S(i) = 0.32(1)$  (Figure 2, centroid···centroid 15.72 Å), and  $S(i) = 0.29(1)$  (Figure 6, centroid···centroid 16.60 Å). The results for these more simple

ensembles were a reminder that the CSM  $S(i)$  method treats an ensemble of two skeletons as one object and calculates the closest theoretical geometry for that ensemble having ideal inversion symmetry within. A size normalization scaling factor is included in these calculations, so that an object's size would not influence its  $S(G)$  value for distortion from an ideal  $G$  symmetry. However, when the “object” is a composite of two molecules/fragments, then the distance between them influences the object's size. Since the four pseudoinversions in our crystal involved pairs of diastereomeric skeletons with different intermolecular distances, the distance normalization function had to be removed from the Continuous Symmetry Measures. This was previously done by Yogev–Einot and Avnir<sup>18</sup> to afford a nearly constant chirality measure that was independent of the length of a quartz helix. Using their modification, atoms in the input ensemble were superimposed on those of the closest theoretical ideal ensemble (coordinates listed in the output file prior to the distance normalization step). Now, the same rms distance value of 0.088(1) Å was calculated for all four skeletal ensembles. We called this  $\text{rms}(i)$

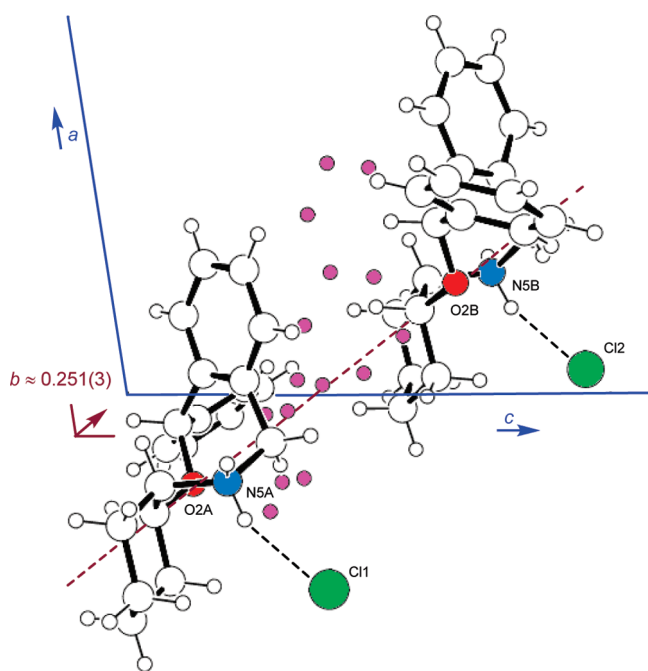


**Figure 7.** Illustration of graphically enlarged magenta colored midpoints (i.e., average coordinates)  $[\bar{x}, \bar{y}, \bar{z}]$  between corresponding  $n$ -pairs of atoms in the approximately enantiomeric fused-ring skeletons of **1**. This array of points represents an almost planar pseudo- $n$ -glide reflection projection  $[y = 0.251(3)]$  between molecules (+)-A $[x - 1, y, z]$  on left-bottom and (-)-B $[1 - x, y - 0.5, 1 - z]$  at right-top. The positive direction of the  $b$ -axis in this figure is toward the viewer.

(a crystallographic pseudoinversion tool) to distinguish it from the standard CSM method. The lower the  $\text{rmS}(i)$  distortion value, the higher is the pseudosymmetry fidelity. To put this  $\text{rmS}(i)$  0.088(1) Å value in perspective, distance normalization was removed from the calculations on the four asymmetric ensembles of phenyl pairs, and the result was a ca. five times higher 0.46(1) Å  $\text{rmS}(i)$  value, that was the same for all ensembles.

**Pseudo- $n$ -Glide Reflection.** The combination of bona fide  $2_1$  screw-rotation acting on the pseudoinversion related molecules affords additional pseudosymmetry, providing that the differently skewed phenyl rings are once again ignored, see Figure 7. The array of  $[\bar{x}, \bar{y}, \bar{z}]$  midpoints between corresponding atoms within the approximately enantiotopic fused-ring skeletons of the (+)-A $[1 - x, y, z]$  and (-)-B $[1 - x, y - 0.5, 1 - z]$  molecules represents an almost planar projection that portrays a pseudo  $n$ -glide reflection. The statistical best plane of these points cuts the  $y$ -axis at 0.251(3), and the rms deviation from the best plane was only 0.009 Å. The  $2_1$  screw-rotation afforded a second pseudo- $n$ -glide reflection plane relating skeletons (-)-B and (+)-A $[2 - x, y + 0.5, 1 - z]$ , and its best plane cuts the  $y$ -axis at 0.751(3).

The directional cosines of the  $\alpha$ ,  $\beta$ , and  $\gamma$  angles that the normal to the best plane made with the positive directions of the coordinate axes were 0.0095, -0.9999, 0.0137. This showed that the normal to the statistical best plane was parallel to the  $a, c$ -cell face and justified treating the pseudoglide reflection as separate translation and reflection components. Observation of the glide relationship showed that it was an  $n$ -glide, with  $x_{\text{mean}}$  0.441(6)  $x$ -unit and  $z_{\text{mean}}$  0.50(1)  $z$ -unit pseudotranslations on the  $a$ - and  $c$ -axes. Transformation of the (-)-B atom coordinates by the  $x_{\text{mean}}$  and  $z_{\text{mean}}$  pseudotranslation values afforded a new ensemble containing a dummy (-)-B molecule opposite to a real (+)-A molecule.

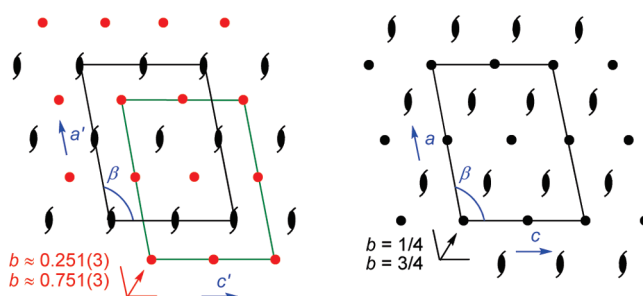


**Figure 8.** Axes of  $2_1$  screw-rotation [colored black] are a feature common to symmetry element diagrams of both the  $P2_1$  ( $Z = 4, Z' = 2$ ) chiral unit cell of **1** (conventional black outline and analogous green on the left) and of a  $P2_1/n$  ( $Z = 4, Z' = 1$ ) achiral unit cell (on the right). The red colored pseudosymmetry elements in the diagram for the  $P2_1$  crystal structure of **1** are located in a spatial arrangement approximating that of the black colored  $P2_1/n$  special positions of inversion and  $n$ -glide reflection symmetry. The positive direction of both  $b$ -axes in this figure is toward the viewer.

The Cartesian coordinates of the closest theoretical ensemble having ideal reflection were extracted from the CSM  $S(\sigma)$  output file. The rms of superimposition of similar atoms in the ideal and input ensembles provided a 0.076(1) Å nondistance normalized  $\text{rmS}(\sigma)$  value (denoted as the crystallographic pseudoreflection tool, to distinguish it from the CSM  $S(\sigma)$ ). To also put this value into quantitative perspective,  $\text{rmS}(\sigma) = 0.91(1)$  Å when just the ensembles of edge-to-face phenyl ring pairs were calculated. As with inversion, the asymmetric ensembles of these phenyl rings are incompatible with  $n$ -glide symmetry.

**Pseudo- $x$ - or  $z$ -Translation.** The difference between an actual  $x_i$ -translation ( $\Delta x_i = x_i(A) - x_i(B)$ ) minus the ideal 0.5 value for a bona fide glide reflection operation (or  $2_1$  screw-rotation) was calculated for each of the  $n$ -pairs of atoms in the ensemble. The rms value for the set of  $n$ -differences is the deviation from an ideal crystallographic  $x$ -translation (in fractional coordinates),  $\text{rmS}(x\text{-translation})_{\text{coordinate}} = 0.059$   $x$ -units. Similarly,  $\text{rmS}(z\text{-translation})_{\text{coordinate}} = 0.013$   $z$ -units. These values were multiplied by the respective 10.224(2) Å  $a$ - or 12.724(2) Å  $c$ -axes cell lengths to give the relevant crystallographic pseudotranslation measures: 0.608 Å  $\text{rmS}(x\text{-translation})$  and 0.160 Å  $\text{rmS}(z\text{-translation})$ . The  $\text{rmS}(n\text{-translation})$  is the 0.38(6) Å average value of the  $\text{rmS}(x\text{-translation})$  and  $\text{rmS}(z\text{-translation})$ . Finally, the 0.45(6) Å  $\text{rmS}(n\text{-glide})$  measurement is the sum of its two components:  $\text{rmS}(\sigma) + \text{rmS}(n\text{-translation})$ : 0.076(1) Å + 0.38(6) Å.

**Pseudosymmetry and Apparent Packing.** Axes of  $2_1$  screw-rotation (colored black) are a feature shared by both an achiral  $P2_1/n$  supergroup cell ( $P2_1/c$  with unique axis  $b$ , cell choice 2 in the *International Tables*,<sup>45</sup> Figure 8 right drawing  $a-0-c$ ) and by a chiral  $P2_1$  cell (with unique axis  $b$ , Figure 8 left drawing  $a'-0'-c'$ ). The special positions of inversion and  $n$ -glide reflection symmetry in this illustration [colored black] in a  $P2_1/n$  crystal have been desymmetrized into approximately located statistical best points  $[0.779(3), 0.501(2), 0.249(4)]$ ,  $[0.221(3), 0.501(2), 0.751(4)]$ ,  $[0.279(3), 0.501(2), 0.249(4)]$ ,  $[0.721(3), 0.501(2), 0.751(4)]$ , and best planes  $[b = 0.251(3)$  and  $b = 0.751(3)]$  of pseudosymmetry [colored red] in  $P2_1$  crystals of **1**. As a result, molecules in the  $P2_1$  crystals were freed from symmetry positional constraints and have slightly realigned themselves for both an optimal fit and for auspicious interactions while their overall space filling still approximates that of the

supergroup. The major significance of this emulation of  $P2_1/n$  space filling is highly efficient packing. Of the 230 space groups, the monoclinic  $P2_1/c$  space group and its glide equivalents are exhibited by more than one-third of all the entries in the CSD.<sup>46</sup>

**Pseudosymmetry and Accuracy.** Intermolecular interactions may be considered to be chemical constraints. The hydrogen-bond ring pattern places the set of molecules (+)-A and (-)-B within close proximity to each other (Figure 2). Another chemical constraint is the aromatic–aromatic interaction which keeps the phenyl centroids in the set of molecules (+)-A[1 -  $x$ ,  $y$  + 0.5, 1 -  $z$ ] and (-)-B[1 -  $x$ ,  $y$  - 0.5, 1 -  $z$ ] also close (Figure 4). The statistically determined best points of pseudoinversion between the almost enantiotopic skeletons in each set of two molecules in the chiral crystal structure are located at the respective positions [0.779(3), 0.501(2), 0.246(4)] and [0.221(3), 0.501(2), 0.751(4)]. Corresponding ideal special positions in an achiral  $P2_1/n$  cell are at [3/4, 1/2, 1/4] and [1/4, 1/2, 3/4] using the same origin. Thus, the pseudosymmetry elements have been *relocated* from ideal positions. The largest deviation in the accuracy of the best points appears to be along the  $a$ -axis (the  $x$ -coordinates). The pseudoinversion point in the hydrogen-bonding set is between the two molecules and is +0.029(3)  $x$ -fractional coordinate units (ca. 0.3 Å) *above* the ideal  $x = 3/4$  location. The pseudoinversion point in the aromatic–aromatic interaction set is also between the two molecules and is -0.029(3)  $x$ -fractional coordinate units (~0.3 Å) *below* the ideal  $x = 1/4$  location. Therefore, pseudoinversion symmetry in the  $P2_1$  lattice has enabled a relative displacement of ca. 0.6 Å along the  $a$ -axis between the two sets of chemically constrained molecules. By Group Theory, this separation is also manifested by the relative large  $\text{rmS}(x\text{-translation})$  of 0.608 Å for the  $n$ -glide.

## CONCLUSIONS

One type of desymmetrization of a space group preserves some of its symmetry operations and converts others into pseudosymmetry relationships. Pseudosymmetry in this false conglomerate allows the larger skeletal fragment and the phenyl ring of the secondary ammonium salt (**1**) to assume different structural roles within the lattice. Low pseudosymmetry measurements of  $\text{rmS}(i) = 0.088$  Å and  $\text{rmS}(\sigma) = 0.077$  Å for the skeletal fragments testify to a high fidelity for the pseudosymmetry operations which interconvert handedness. As a result, the two spatially demanding skeletons of opposite handedness in the asymmetric unit of **1** emulate a  $P2_1/n$  higher order packing efficiency and hydrogen bonding, while symmetry breaking aromatic–aromatic interactions are simultaneously allowed to exist.

## ASSOCIATED CONTENT

**S Supporting Information.** A CIF file, scheme, and synthesis details of salt **1**, seven tables of crystal data and structure refinement, non-hydrogen atomic coordinates and equivalent isotropic displacement parameters, bond lengths and angles, anisotropic displacement parameters, hydrogen coordinates and isotropic displacement parameters, torsion angles, and hydrogen-bonds for **1**, explanation of the Avnir CSM calculation, and Figure 9 showing the deviation of a distorted  $C_{3h}$  structure from one of ideal  $C_3$  symmetry. This material is available free of charge via the Internet at <http://pubs.acs.org>.

## AUTHOR INFORMATION

### Corresponding Author

\*E-mail: [rglaser@bgu.ac.il](mailto:rglaser@bgu.ac.il)

## ACKNOWLEDGMENT

This work would not have been possible without the generosity of Prof. David Avnir (Hebrew University of Jerusalem) who provided us with access to his CSM and Error Estimation Programs. The authors express their gratitude to him and his co-workers for their warm encouragement and kindness.

## REFERENCES

- (1) Guijarro, A.; Yus, M. In *The Origin of Chirality in the Molecules of Life*; The Royal Society of Chemistry: The United Kingdom, 2009; pp 150.
- (2) Eliel, E. L.; Wilen, S. H.; Mander, L. N. In *Stereochemistry of Organic Compounds*; John Wiley & Sons: New York, 1994; pp 1267.
- (3) Desiraju, G. R. *Cryst. Eng. Chem.* **2007**, *9*, 91.
- (4) Allen, F. H. *Acta Crystallogr. B* **2002**, *58*, 380.
- (5) Steed, J. W. *Cryst. Eng. Chem.* **2003**, *5*, 169.
- (6) Bishop, R.; Scudder, M. L. *Cryst. Growth Des.* **2009**, *9*, 2890.
- (7) Gavezzotti, A. *Cryst. Eng. Chem.* **2008**, *10*, 389.
- (8) Zabrodsky, H.; Peleg, S.; Avnir, D. *J. Am. Chem. Soc.* **1992**, *114*, 7843.
- (9) Zabrodsky, H.; Peleg, S.; Avnir, D. *J. Am. Chem. Soc.* **1993**, *115*, 8278.
- (10) Avnir, D.; Katzenelson, O.; Keinan, S.; Pinsky, M.; Pinto, Y.; Salomon, Y.; Zabrodsky, H. *The Measurement of Symmetry and Chirality: Conceptual Aspects*; Rouvray, D. H., Ed.; Research Studies Press: Taunton, England, 1997; pp 283.
- (11) Pinsky, M.; Avnir, D. *Inorg. Chem.* **1998**, *37*, 5575.
- (12) Pinsky, M.; Yogeve-Einot, D.; Avnir, D. *J. Comput. Chem.* **2003**, *24*, 786.
- (13) Pinsky, M.; Dryzun, C.; Casanova, D.; Alemany, P.; Avnir, D. *J. Comput. Chem.* **2008**, *29*, 2712.
- (14) Pinsky, M.; Casanova, D.; Alemany, P.; Alvarez, S.; Avnir, D.; Dryzun, C.; Kizner, Z.; Sterkin, A. *J. Comput. Chem.* **2008**, *29*, 190.
- (15) Zabrodsky, H.; Avnir, D. *J. Am. Chem. Soc.* **1995**, *117*, 462.
- (16) Cirera, J.; Alemany, P.; Alvarez, S. *Chem.—Eur. J.* **2004**, *10*, 190.
- (17) Alvarez, S.; Avnir, D.; Lluell, M.; Pinsky, M. *New J. Chem.* **2002**, *26*, 996.
- (18) Yogeve-Einot, D.; Avnir, D. *Chem. Mater.* **2003**, *15*, 464.
- (19) Alvarez, S.; Alemany, P.; Avnir, D. *Chem. Soc. Rev.* **2005**, *34*, 313.
- (20) Yogeve-Einot, D.; Avnir, D. *Tetrahedron: Asymmetry* **2006**, *17*, 2723.
- (21) Steinberg, A.; Karni, M.; Avnir, D. *Chem.—Eur. J.* **2006**, *12*, 8534.
- (22) Dryzun, C.; Mastai, Y.; Shvalb, A.; Avnir, D. *J. Mater. Chem.* **2009**, *19*, 2062.
- (23) Dryzun, C.; Avnir, D. *Phys. Chem. Chem. Phys.* **2009**, *11*, 9653.
- (24) Saragusti, I.; Sharon, I.; Katzenelson, O.; Avnir, D. *J. Archeol. Sci.* **1998**, *25*, 817.
- (25) Echeverria, J.; Alvarez, S. *Inorg. Chem.* **2008**, *47*, 10965.
- (26) Cirera, J.; Ruiz, E.; Alvarez, S. *Organometallics* **2005**, *24*, 1556.
- (27) Alvarez, S. *Dalton Trans.* **2005**, 2209.
- (28) Alvarez, S.; Alemany, P.; Avnir, D. *Chem. Soc. Rev.* **2005**, *34*, 313.
- (29) Echeverria, J.; Casanova, D.; Lluell, M.; Alemany, P.; Alvarez, S. *Chem. Commun.* **2008**, 2717.
- (30) Collins, A.; Cooper, R. I.; Watkin, D. J. *J. Appl. Crystallogr.* **2006**, *29*, 842.
- (31) Kroumova, E.; Aroyo, M. I.; Perez-Mato, S.; Ivantchev, J. M.; Wondratschek, H. *J. Appl. Crystallogr.* **2001**, *31*, 783.

- (32) Igartua, J. M.; Aroyo, M. I.; Perez-Mato, J. M. *Phys. Rev. B* **1996**, *54*, 12744.
- (33) Capillas, C.; Aroyo, M.; Perez-Mato, J. M. *Z. Kristallogr.* **2005**, *220*, 691.
- (34) Glaser, R.; Geresh, S.; Blumenfeld, J.; Donnell, D.; Sugisaka, N.; Drouin, M.; Michel, A. *J. Pharm. Sci.* **1993**, *82*, 276.
- (35) The atomic coordinates for salt **1** have been deposited in the Cambridge Structural Database, Cambridge Crystallographic Data Centre, Cambridge CB2 1EZ, United Kingdom.
- (36) *SAINTE*, version 6.45a; Bruker AXS Inc.: Madison, WI, 2004.
- (37) Sheldrick, G. M. *SADABS*; University of Göttingen, Germany, 2004.
- (38) Sheldrick, G. M. *SHELXTL*, version 5.1; Bruker AXS Inc.: Madison, WI, 1999; Sheldrick, G. M. *Acta Crystallogr.* **2008**, *A64*, 112.
- (39) <http://www.csm.huji.ac.il/new/?cmd=symmetry.23&act=adv>.
- (40) *MATLAB*, version R2010a; The Math Works: Natick, MA, 2010.
- (41) Smith, I. *LSPLANE*, version 2.02; 2002 and *LSPLANE*, version 2.02; 2002 are programs in the LEAST SQUARES GEOMETRICAL ELEMENTS (LSGE) library for *MATLAB*. The *LSGE-MATLAB.zip* file is available free of charge via the Internet at [http://www.eurometros.org/file\\_download.php?file\\_key=66](http://www.eurometros.org/file_download.php?file_key=66).
- (42) Glaser, R.; Cohen, S.; Donnell, D.; Agranat, I. *J. Pharm. Sci.* **1986**, *75*, 772.
- (43) Bernstein, J.; Davis, R. E.; Shimoni, L.; Chang, N. L. *Angew. Chem., Int. Ed. Engl.* **1995**, *34*, 1555.
- (44) Burley, S. K.; Petsko, G. A. *Science* **1985**, *229*, 23.
- (45) Hahn, T., Ed. *International Tables of Crystallography*; International Union of Crystallography, Kluwer Academic Publishers: Dordrecht, the Netherlands, 2002; Vol. A, p 120 and 187.
- (46) Yao, J. W.; Cole, J. C.; Pidcock, E.; Allen, F. H.; Howard, J. A. K.; Motherwell, W. D. S. *Acta Crystallogr. B* **2002**, *58*, 640.